Eng. Sci., 2025, **33**, 1319

Engineered Science
DOI: https://dx.doi.org/10.30919/es1319

Flavonoids Isolation from *Stellera Chamaejasme* for Preparing Antimildew and Anti-decay Soybean Protein Isolate-based Adhesives

Min Pan,[1,#] Shuliang Li,[2,#] Shengtao Yang,[1,*] Xinyi Dong,[2] Xiaoliang Wang,[2] Ting Huang,[2] Yihui Wu,[1] Yuanhu Tuo[1] and Xianmin Mai [2,*]

Abstract

Renewable bio-based adhesives help to address environmental pollution, non-renewable petrochemical resources usage and formaldehyde emissions in the wood-based panel industry. Soybean protein isolate (SPI) adhesive has great potential to replace formaldehyde-based adhesive, but it has problems such as poor antibacterial effect, poor water resistance, weak adhesive strength, and high brittleness. This work has extracted the active substance (SE), which contains flavonoids, and derived cellulose nanocrystals (CNC) from the roots of *Stellera chamaejasme*. The SPI lateral chains amino groups react with flavonoids in SE under alkaline conditions; the incorporation of flavonoids rather than widely used tannin with SPI results in the desired crosslinking efficiency and satisfied interfacial adhesion, while the crosslinking agent oligo(ethylene glycol) hydrazine derivative (BHTA) with multiple epoxy groups undergoes a ring-opening reaction to form a waterproof multiple cross-linked network. Mineralized CNC can improve the adhesive's load transfer and energy dissipation capabilities and introduce metal coordination to enhance the toughness and bonding strength of SPI adhesives. These synergistic effects significantly improve the water resistance and bonding strength. Consequently, the dry and wet bonding strength are 4.19 MPa and 1.17 MPa, respectively. Furthermore, this novel adhesive performs excellent anti-decay and anti-mold effects. Therefore, this study could guide the future development of bio-adhesive materials.

Keywords: Flavonoid; Bio-adhesive; Anti-decay effect; Multiple crosslinking; *Stellera chamaejasme.*
Received: 06 September 2024; Revised: 04 November 2024; Accepted: 11 November 2024.
Article type: Research article.

1. Introduction

Plywood is widely used, and the vast majority of their adhesives are based on non-renewable petroleum and formaldehyde such as urea formaldehyde (UF), phenol-formaldehyde (PF), resorcinol formaldehyde (RF) and melamine formaldehyde (MF).[1] However, this type of adhesive has obvious drawbacks as it releases carcinogenic formaldehyde gas, phenol, toluene, *etc*.[2] Therefore, it is necessary to develop new green adhesives using renewable biomass resources as raw materials. Bio-adhesives mainly composed of soybean protein,[3] tannins,[4] lignin, and cellulose[5] have been developed. Among them, soybean protein has been widely studied due to its low cost and high processability.[6] However, soybean protein-based adhesive exhibited inferior adhesive strength, poor water resistance, high brittleness and weak resistance to microorganisms.[7]

Nowadays, alkali thermal modification, soy protein structure denaturant, branching,[8] crosslinker,[9] nanomaterial filling,[10] biomimetic design,[11] biomineralization and enzymatic hydrolysis[12] have been proven to be effective to solve the above-mentioned shortcomings of protein adhesives. Specifically, alkali thermal modification can alter the structure and viscosity of soybean protein, reduce its molecular size, and significantly improve its dry binding performance.[13] Biomineralization can be achieved through the rational combination of organic components and inorganic minerals.[14] Graphene,[15] boron nitride nanosheets,[16] amino clay, mineralized cellulose nanocrystals (CNC),[17] montmorillonite,[18] *etc.* were introduced into soybean protein adhesives to improve the cohesion of adhesives and provide

[1] *School of Chemistry and Environment, Southwest Minzu University, Chengdu, 610041, China*
[2] *School of Architecture, Southwest Minzu University, Chengdu, 610041, China*
[#] *These authors contributed equally to this work.*
**Email:* maixianmin@swun.edu.cn (X. M. Mai), yangst@pku.edu.cn (S. T. Yang)

other functions like mildew resistance. However, a single modification method is limited in updating the performance of soybean protein adhesives, and a rational design of multiple modification methods is required to obtain better-behaved adhesives.

Due to the growing awareness of environmental pollution and resource exhaustion, taking advantage of the highest possible percentage of renewable biomass-derived materials to minimize or even avoid petroleum-derived chemicals has gradually become a new research hotspot. Tannin, as a natural polyphenol compound, can be generally divided into hydrolyzed tannin and condensed tannin, among which condensed tannin is often used as the wood adhesive to exert its phenolic properties or advantages in the number of hydroxyl groups. Condensed tannins are flavan 3-ols as monomers and their polymers. Recently, adhesives from only soy protein and tannin have shown the potential of preparing effective plywood wood panel adhesives. However, the molecular weight of condensed tannin is too large, and tannin-derived adhesives are often faced with problems such as low crosslinking reactivity and uneven reaction. Biomass-derived polyphenols have been proven to react with the protein lateral chains amino or mercapto groups and are used as cross-linking agents for gelatin gel.[19] The phenolic hydroxyl group is oxidized to quinone derivative through its radical intermediate, which can subsequently react with electron-dense groups in proteins such as amino or thiol groups to induce covalent cross-linking.[20] Flavonoids contain a large amount of phenolic hydroxyl groups.[21] Proteins are expected to react more covalently with flavonoids as flavonoids have more reaction sites and higher crosslinking efficiency compared with tannins.[22] Thus, in this work, flavonoids, which are widely found in natural plants, are chosen to modify soy adhesives for wood panels.

Stellera chamaejasme L is a type of Chinese herbal medicine that grows on the western Sichuan Plateau and is also a raw material for Tibetan paper. It has therapeutic effects on edema,[23] fungal infections,[24] and cancer.[25] Its roots contain a large amount of antibacterial active ingredients such as flavonoids,[26] tannin, lignans,[24] terpenoids,[27] and coumarins,[25] *etc*. Flavonoids (Dihydro flavones, Chamaechromone, Rutin, and so on) in the extract of *Stellera chamaejasme* (Fig. 1) can act as crosslinking agents to react with soy protein isolate and achieve desired crosslinking efficiency and satisfactory interfacial adhesion. Other active substances, such as coumarins and lignans, can enhance the anti-decay and anti-mold performance of soybean protein isolate (SPI).

Here, we report a facile, green, and scalable biomass-derived adhesive. The adhesive is yellow brown in color and when used alone, it affects the appearance of the wood. Therefore, it is more suitable for preparing plywood. The plywood prepared with this adhesive does not release formaldehyde, and its wet shear strength meets the standard of Class II plywood, making it suitable for indoor use, especially in damp indoor locations.

As shown in Scheme 1, active substance (SE) which contains flavonoids and CNC are from the roots of *Stellera chamaejasme*, and the extracted flavonoids subsequently react with SPI. The SPI lateral chains such as amino groups substitute some of the phenolic hydroxyl groups of the flavonoids in SE under alkaline conditions to form a covalent cross-linked network. An active biomineralized skeleton (M-CNC), which is achieved by the deposition of calcium carbonate on the surface of CNC, is incorporated to improve the adhesive's load transfer and energy dissipation capabilities and introduce metal coordination to enhance the toughness and bonding strength of SPI adhesives. The added crosslinking agent oligo(ethylene glycol) hydrazine derivative (BHTA, abbreviated as B) with multiple epoxy groups undergoes a ring-opening reaction to react with the hydrophilic hydroxyl and amino groups of SPI molecules and forms a multiple crosslinking network with SPI, SE, and M-CNC. These synergistic effects of hydrogen bonds, covalent bonds, and metal coordination significantly improve the water resistance and cohesive strength of the adhesive.

Meanwhile, antibacterial active substances from SE can endow the adhesive with anti-decay and anti-mold effects, and the charge effect of mineralized CNC further enhances this effect. It is worth noting that in this study, Flavonoids, rather than tannins or flavonoids grafted with epoxy groups, were first used as crosslinking agents. And the antibacterial active substances in the roots of *Stellera chamaejasme* were used to endow SPI-based adhesives with anti-decay and anti-mold properties. At the same time, the fibers and active components in the roots of the wolf venom plant are fully utilized, achieving its high-value application. This study will provide ideas for the preparation of antibacterial and anti-corrosion SPI-based adhesives and the utilization of toxic plants.

2 Materials and methods

2.1 Materials

Stellera chamaejasme L was collected from the western Sichuan Plateau. The type of soy protein isolate was Songshan Biology, type 100. Concentrated sulfuric acid (98%) and ethanol (95%), were purchased from Cologne Chemical Reagents Co., Ltd. Triethylenetetramine (>65%) and 1,6-hexanediol diglycidyl ether (epoxy value: 0.65~0.70) were purchased from Aladdin. Calcium chloride (96%) and anhydrous sodium carbonate (99.5%) were purchased from Macklin. The PDA culture medium was purchased from Solarbio. White rot fungi and *Trichoderma harzianum* were purchased from Guangdong Provincial Microbial Species Preservation Center. Populus (300 mm × 300 mm × 2 mm) and tung (500 mm × 100mm × 1.5 mm) wood boards were purchased from Shijiazhuang, Hebei.

2.2 Extracting active constituents from the roots of *Stellera chamaejasme*

The roots of *Stellera chamaejasme* were crushed, soaked in

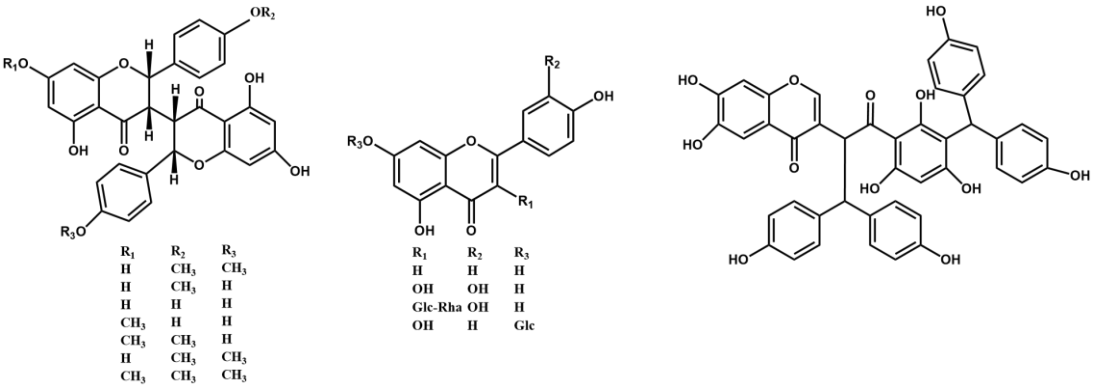

Fig. 1: Structural formula of some polyphenol compounds in the extract of *Stellera chamaejasme*.[28]

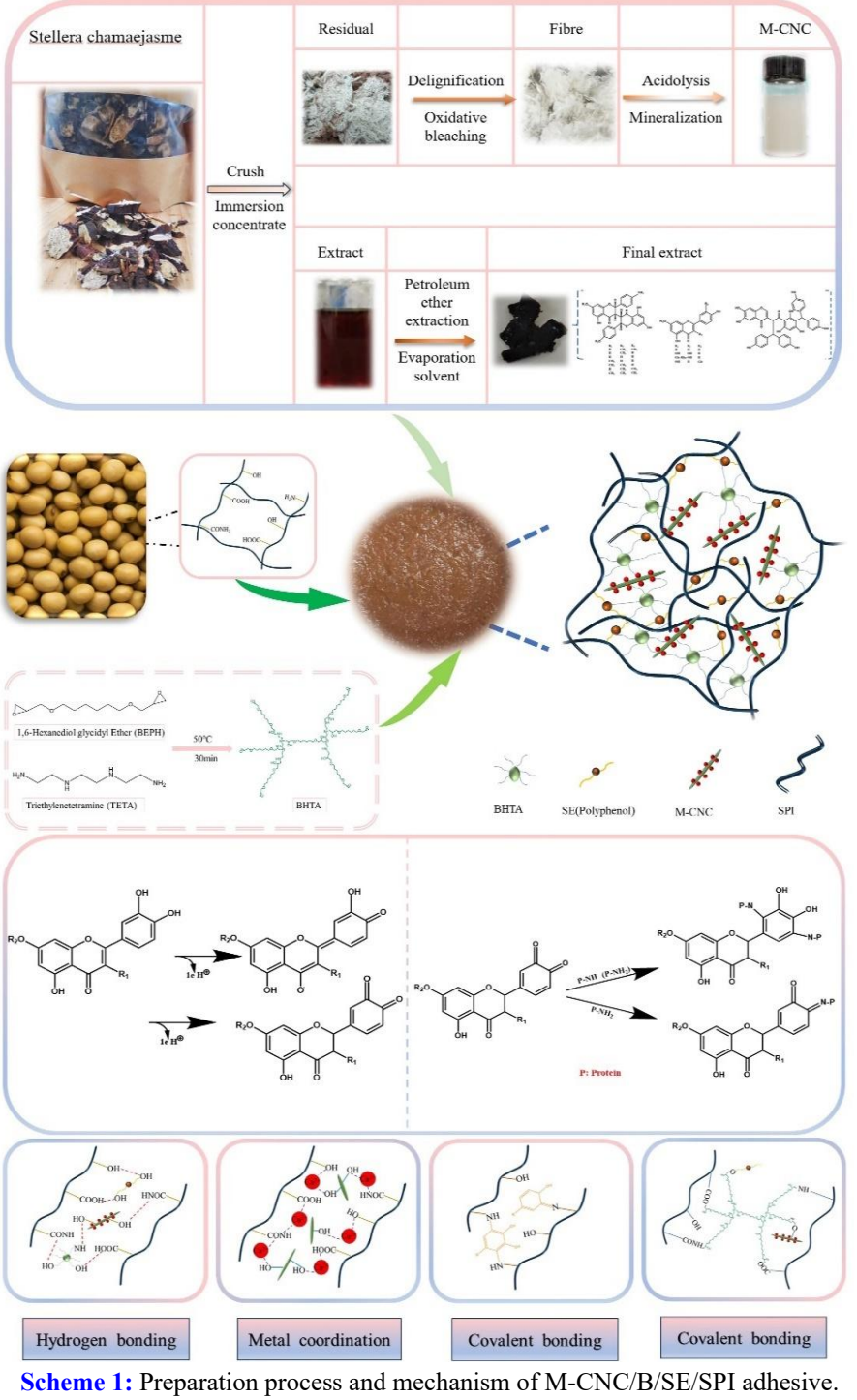

Scheme 1: Preparation process and mechanism of M-CNC/B/SE/SPI adhesive.

ethanol, and sonicated for 1 hour. Then, the mixture was poured into a larger container, mixed with ethanol with a solid-liquid ratio of 1:10, and soaked for 10 days. The impregnation solution was concentrated to a dark brown viscous liquid using a rotary evaporator. Finally, the oil-soluble components were removed using petroleum ether, and all solvents were evaporated to obtain a reddish-brown solid (Scheme 1). A standard curve was drawn using rutin as the standard substance (Fig. S2), and the total flavonoid content in the root extract of *Stellera chamaejasme* was determined.[29] The total flavonoid content was 11.21%.

2.3 Preparation of additives

2.3.1 Crosslinker

1,6-hexanediol diglycidyl ether reacted with triethylenetetramine with a mass ratio of 10:1 at 50 ℃ for 30 min[30] to obtain BHTA. The reaction is shown in Scheme 1.

2.3.2 Mineralized CNC (M-CNC)

Cellulose was derived from the roots of *Stellera chamaejasme* with a yield of 15.02%. The extraction process could be found in Supporting information S1. Then, CNC was prepared via sulfuric acid hydrolysis (Supporting information S2). Referring to the work of Li Kuang *et al*,[17] an equal amount of $CaCl_2$ was dissolved in a 5 wt% CNC solution, stirred for 1 hour. Then, an equal amount of Na_2CO_3 was added, reacted for 2 h, and precipitated by suction filtration to obtain M-CNC (Scheme 2).

2.4 Preparation of adhesive

One-step blending was used to prepare M-CNC/B/SE/SPI adhesives. SE was added to water, pH of the solution was adjusted to 9.5, BHTA and M-CNC were added subsequently. The mixture was reacted for 15 minutes at 70 ℃. The specific ratio was shown in Table 1.

2.5 Characterization

The adhesive samples SPI, SE/SPI, B/SE/SPI, M-CNC/B/SE/SPI were scanned using Fourier-transform infrared (Elemental Germany) spectroscopy with a 4cm^{-1} resolution in the range of 500 to 4000 cm^{-1} to analyze changes in functional groups of the samples. And the chemical structures of four adhesives also were analyzed using X-ray diffractometer (XRD, Ultima IV, Rigaku, Japan) with a Cu-Ka radiation source and diffraction angles ranging from 5° to 60°. X-ray photoelectron spectroscopy (XPS) was performed using an XPS spectrometer (Thermo SCIENTIFIC ESCALAB 250Xi USA) at a resolution of 0.1 eV at 50 eV. The cross-sectional morphology of the cured adhesive film was observed using scanning electron microscope (SEM Thermo Quattro S USA). Atomic force microscopy (AFM) was used to observe the microstructure of M-CNC with a scanning range of 1-5 μm.

2.6 Crack observation

The toughness of adhesives was evaluated by the occurrence of cracks after curing. The adhesive samples were evenly coated on the glass slides and then dried in an oven at 120 ℃ for 2 h. The cured adhesives were photographed with a digital camera to observe crack conditions and analyze samples' toughness.

2.7 Sol-gel test

The initial weight (M_1) was measured. Subsequently, the weighed adhesive samples were immersed in excessive boiling water for 3 h. After filtering through a 200 mesh sieve, the adhesives were dried until reaching a constant weight (M_2). The insoluble fraction was then calculated using the following Eq. (1):

$$Insoluble\ fraction\ (\%) = \frac{M_2}{M_1} \times\ 100\% \qquad (1)$$

Table 1: Proportions of adhesives.

Sample entry	Proportion
SPI	M(SPI): M(Water)=12:84
SPI/SE	M(SPI): M(Water):M(SE)=12:84:3.6
SPI/SE/BHTA	M(SPI): M(Water):M(SE):M(BHTA)=12:84:3.6:2.4
SPI/SE/BHTA/M-CNC	M(SPI): M(Water):M(SE):M(BHTA): M(M-CNC)=12:84:3.6:2.4:1.8

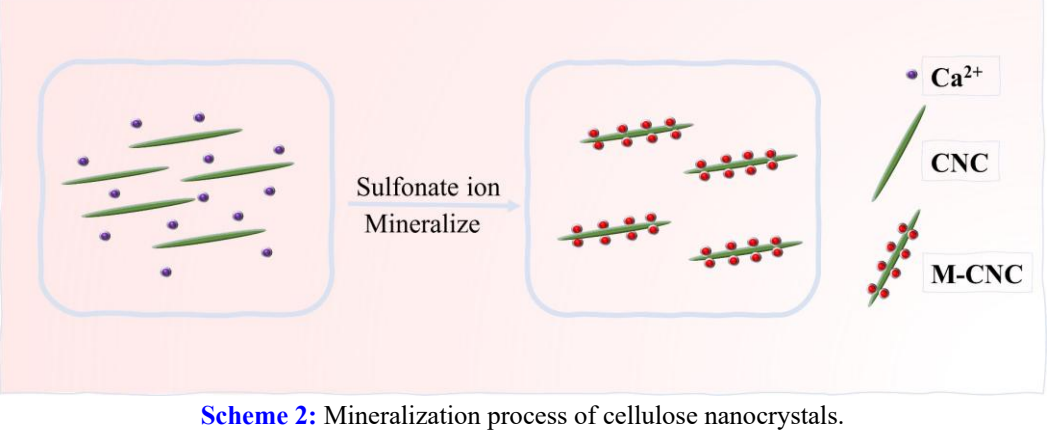

Scheme 2: Mineralization process of cellulose nanocrystals.

2.8 TG analysis of adhesives

The thermogravimetric analysis of the adhesives was conducted in N_2 atmosphere (NETZSCH STA449Germany), with a heating rate of 10 ℃/min. The temperature range for testing was between 60 ℃ and 600 ℃.

2.9 Shear strength measurements

The adhesives were evenly brushed on the surface of the poplar board with a dosage of 200-220 g/m^2. The two boards were combined and pressed at 1.5 MPa and 105 ℃ for 3 min to prepare plywood. Before testing the bonding strength, the plywood should be left at room temperature for 24 h. Then, the plywood was cut into specimens (100 mm × 25 mm).

The bonding strength of plywood was tested according to the Chinese national standard (GB/T17657-2013). The universal testing machine (CMT6502 Jinan) was used to test the dry and wet shear strength of specimens at a loading speed of 10 mm/min. The stress situation was shown in Scheme 3. Before testing the wet shear strength, the samples needed to be soaked in hot water at 63 ℃ for 3 h and then air dried for 10 min. Each group was tested six times.

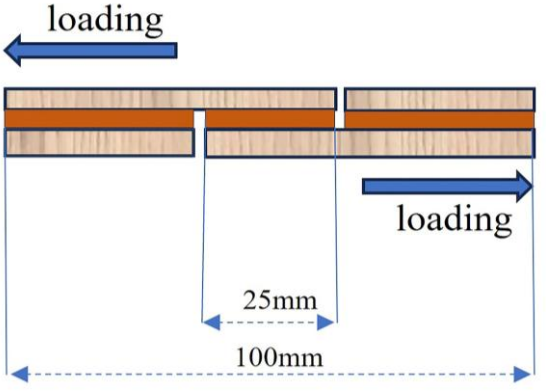

Scheme 3: The stress situation during the sample testing process.

2.10 Antimildew and antifungal properties

6 g adhesive was evenly spread in a culture dish with a diameter of 6 cm, and then placed in an environment at 32 ℃ and 75% RH. The condition of the adhesives, including odor and appearance, was observed and recorded daily. Based on previous studies, we found that *Stellera chamaejasme* had inhibitory effects on various fungi, this study further explored the resistance of adhesives to white rot fungi and *Trichoderma*. 15 g adhesive was added to 60 mL PDA culture medium to prepare a solid culture medium. 5-6 mm fungal block was inoculated onto solid culture medium and incubated in a 28 ℃ incubator for 5 days. The mycelial growth diameter was measured using the cross over method and the growth inhibition rate was calculated according to the following Eq. (2):[31]

$$G = \frac{(d_B - d_T)}{d_B} \times 100\% \quad (2)$$

where G is the growth inhibition rate (%), d_B is the diameter of blank sample (mm), and d_T is the diameter of the treated sample (mm). The diameter of the mycelium in the culture medium with SPI adhesive added was d_B.

2.11 Mechanical properties of plywood

According to the national standard GB/T17657-2013, a three-point bending mechanical test was conducted on the bonded three-layer tung wood plywood to investigate the effect of different adhesives on the mechanical properties of the plywood. The sample size was 50 mm × 5 mm × 3.5 mm, with a support spacing of 20 mm. The calculation formula for static bending strength is as follows in Eq. (3):

$$\delta = \frac{3 \times Fmax \times L}{2 \times b \times t^2} \quad (3)$$

where δ is the static bending strength of the sample (MPa), F_{max} is the maximum load during pattern failure (N), L is the support spacing (mm), b is the specimen width (mm), and t is the style thickness (mm)

3. Results and discussion

3.1 Characterization of M-CNC

The microstructure characteristics of pristine CNC and M-CNC nanoparticles were analyzed by AFM images (Fig. S1). The rod-like fragments of CNC were uniformly dispersed and approximately 500 nm in length. In the height-profile image, CNC was approximately 3.5 nm thick. Additionally, the thickness of the M-CNC segment increased to approximately 10.5 nm. This increase in thickness was attributed to the biomineralization-induced formation of an inorganic mineralization layer on the M-CNC nanoparticles.

3.2 Characterization of adhesives

It was necessary to analyze the impact of modification treatment on the chemical structure of SPI by analyzing the characterization results of the adhesives. This would help to understand the physical and chemical interactions that occur between various components in the adhesives.

3.3 Fourier transform infrared spectrometer (FTIR)

FTIR spectroscopy was used to analyze interactions within adhesives. As shown in Fig. 2a, the broad peak observed at 3454 cm^{-1} was attributed to free and bound N-H and O-H groups.[32] Alkali heat treatment disrupted the secondary structure of SPI, exposing more active groups. Besides, SE contained more phenolic hydroxyl groups. Thus, compared to SPI adhesive, the absorption at 3454 cm^{-1} of SE/SPI, B/SE/SPI, and M-CNC/B/SE/SPI was enhanced. The absorption peaks at 2977 cm^{-1} and 2936 cm^{-1} were C-H symmetric and asymmetric stretching of - CH_2 and - CH_3 groups. 1663 cm^{-1}, 1524 cm^{-1}, and 1234 cm^{-1} were typically characteristic absorption peaks of amide I (C=O stretching), amide II (N-H bending), and amide III (C-N and N-H stretching), respectively.[33] A peak corresponding to the COO-stretching vibration of hydroxyl groups bonded to carbon atoms was observed at 1403 cm^{-1}. The absorption peak at 1071 cm^{-1} was a characteristic peak of

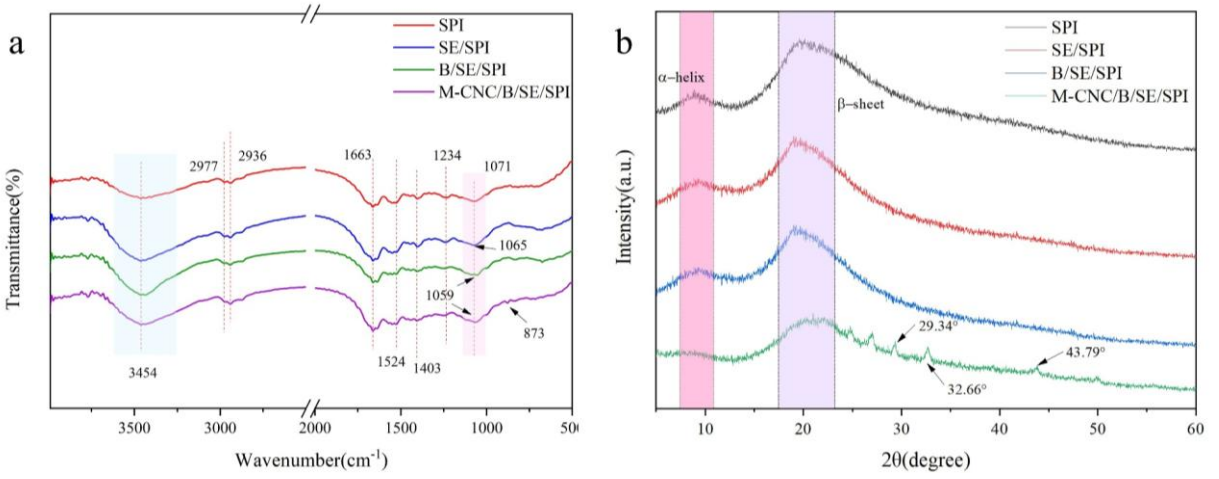

Fig. 2: FTIR (a) and XRD (b) spectra of adhesives.

C-O-C. It was worth noting that due to the Michael addition and Schiff base reaction of polyphenols in SPI and SE under alkaline conditions, as well as the ring-opening reaction of epoxy groups from crosslinking agent with hydroxyl and amino groups of SPI molecules, the absorption peak at 1524 cm^{-1}, 1403 cm^{-1},1234 cm^{-1} gradually weakened,[30,34] the absorption peak at 1071 cm^{-1} enhanced.[35] The absorption peak at 873 cm^{-1} was a characteristic peak of CO_3^{2-} in M-CNC. The red or blue shift of the absorption peak of the functional group proved the existence of various hydrogen bonds.[36] The FTIR results demonstrated the formation of hydrogen bonds, as well as covalent bonds of M-CNC/B/SE/SPI adhesive.

3.4 X-ray diffractometer (XRD)

Crosslinking could alter the conformational structure of protein chains in cured adhesives. The original SPI adhesive had broad diffraction peaks at 19.6 ° and 8.9 °, corresponding to the β-sheet and α-helix structure of the SPI secondary conformation, respectively. Compared with SPI (Fig. 2b), the peak of SE/SPI shifted to a lower degree and became sharp, with a weakened peak intensity,[16,37] implying the reaction between polyphenols of *Stellera chamaejasme* and SPI. The addition of M-CNC completely changed the secondary structure of the protein. The α-helix peak completely disappeared, and β-sheet peak significantly weakened. And new peaks at 29.34°, 32.66°, 43.79° corresponding to calcite appeared in M-CNC\B\SE\SPIA adhesive, implying that M-CNC and SPI were well linked to achieve the toughness of mineral reinforced adhesives.[17]

3.5 X-ray photoelectron spectroscopy (XPS)

Further analysis of the internal structure of the adhesive was conducted using XPS. Compared with pristine SPI, the addition of SE and BHTA significantly increased the content of C-N and C-O in the modified adhesive, indicating successful crosslinking reactions (Figs. a, e, and h). An additional peak appeared at 398.58 eV, which was derived from =N-, as well as the increase in the -NH- area was attributed to Michael addition and Schiff base reaction between the amino groups of SPI and flavonoids of SE (Figs. 3b, f, h, and i).[38] The XPS spectrum of M-CNC/B/SE/SPI adhesive exhibited new peaks (Fig. 3k), which were derived from the Ca 2p of the mineralized CNC, and a new peak at 533.54 eV was associated with Ca-O (Fig. 3j), indicating the formation of an inorganic-organic hybrid composite system between mineralized CNC and SPI.[39]

3.6 Cross section morphology of adhesive

The fracture surfaces of the cured adhesive film were observed through SEM to further investigate the internal interaction force and structural features. As shown in Fig. 4a, SPI adhesive exhibited a flat and smooth surface. Evident holes indicated that interfacial interactions in SPI were relatively weak. After adding SE, the fracture surface became rougher with some evident microcracks due to the cross-linking effect of polyphenol from *Stellera chamaejasme*, indicating the enhanced cohesion by constructing a compact structure of the composite adhesive (Fig. 4b). After the addition of BHTA, the cracks became denser and continuous, implying a stronger and more stable adhesion structure (Fig. 4c). After incorporating M-CNC, the fracture surface displayed evident crack bridges, suggesting an enhanced anchoring effect during the fracture process and the enhanced toughness of the adhesive.[17,40]

3.7 Crack observation

The cracks of different adhesives were observed (Fig. 5) to evaluate their toughness. A large number of small cracks and gas holes were observed in the SPI adhesive due to the inherent brittleness of the protein.[7] The cracks and gas holes provided access for water to infiltration, resulting in poor water resistance. After adding SE, the surface of the SE/SPI adhesive became smooth. But cracks and adhesive aggregation still existed. The morphology of B/SE/SPI was improved by the addition of crosslinker with multiple epoxy groups and flexible long chains, indicating that crosslinking could improve the toughness of the adhesive, but the effect was limited. M-CNC/B/SE/SPI film was smooth with no cracks due to the interface effects of M-CNC nanofillers. The

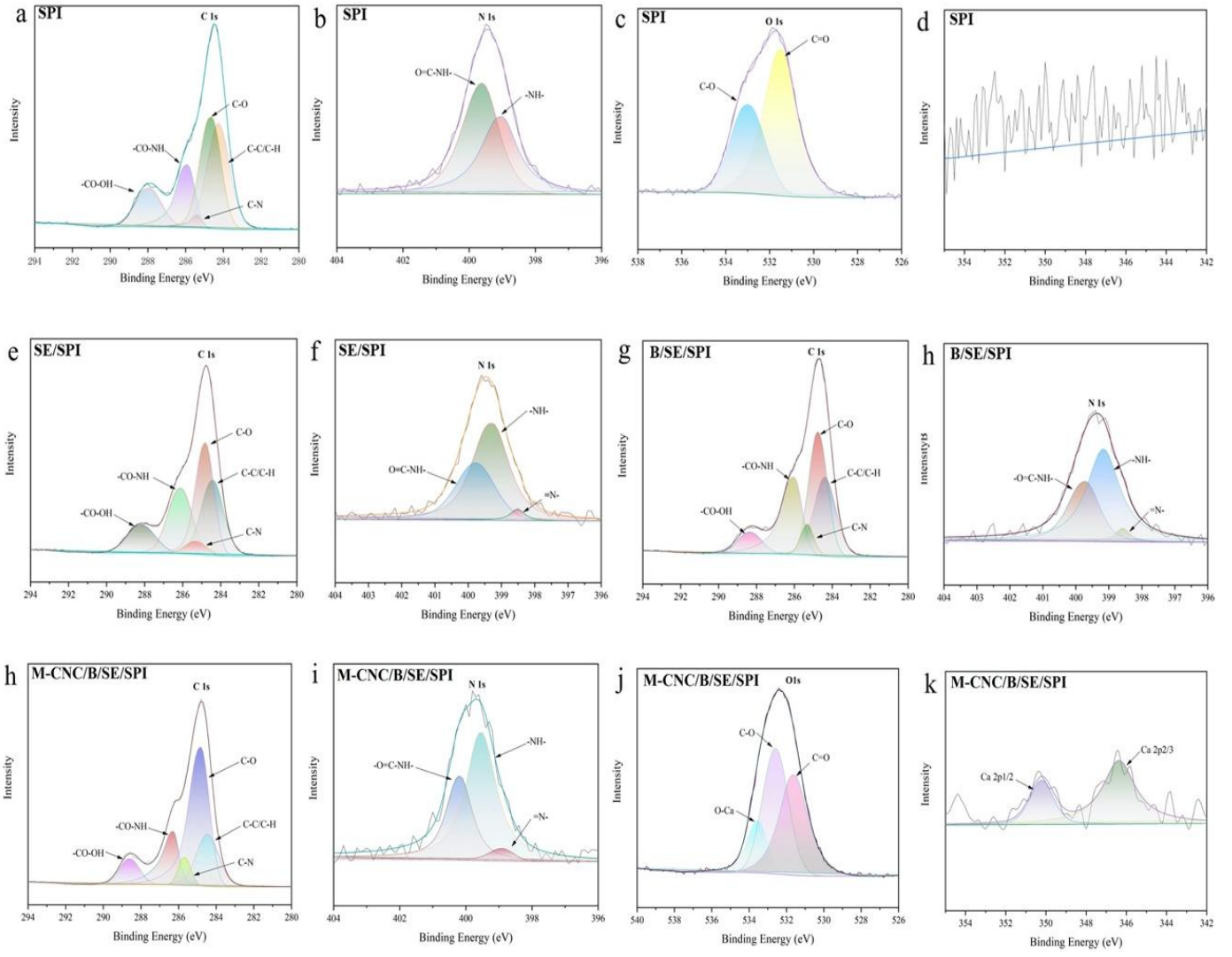

Fig. 3: XPS C 1s spectra of SPI (a), SE/SPI (e), B/SE/SPI (g), M-CNC/B/SE/SPI (h), N 1s spectra of SPI (b), SE/SPI (f), B/SE/SPI (h), M-CNC/B/SE/SPI (i), O1s spectra of SPI (c), M-CNC/B/SE/SPI (j), Ca 2p spectra of SPI(d), and M-CNC/B/SE/SPI (k).

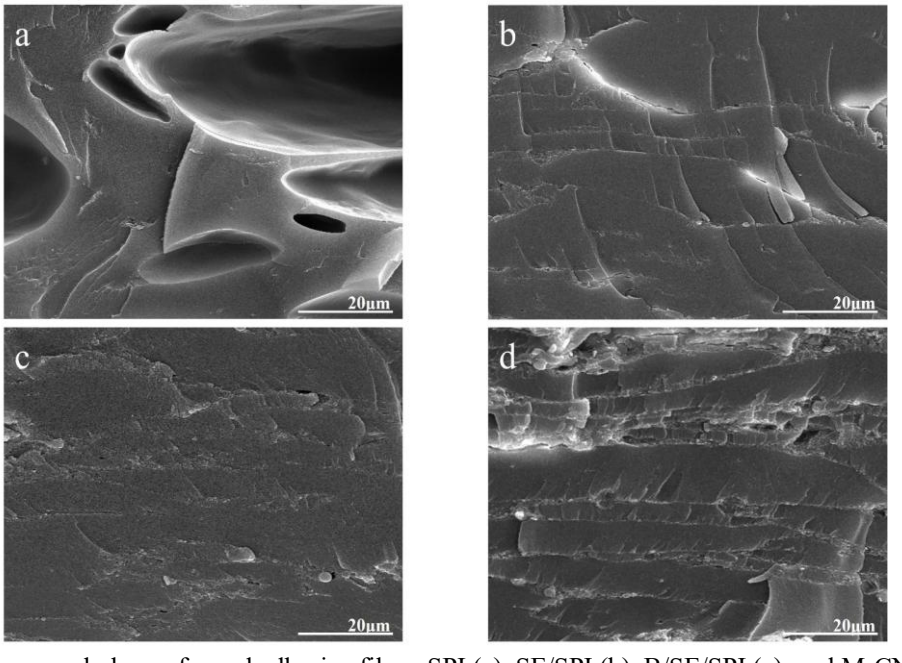

Fig. 4: Cross section morphology of cured adhesive films, SPI (a), SE/SPI (b), B/SE/SPI (c), and M-CNC/B/SE/SPI (d).

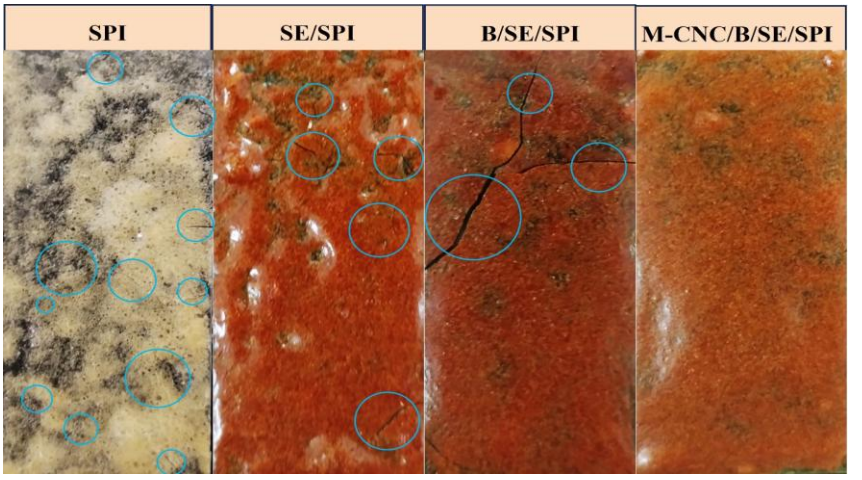

Fig. 5: Digital photos of adhesive films.

toughness of the organic-inorganic hybrid composite formed is significantly improved and strong water resistance was achieved because of the lack of access for water to permeate and corrode.[17]

3.8 Water resistance and thermal performance of adhesives

The hydrophilicity of soybean protein, as well as hydrogen bonding made the interactions between protein and wood easy to be broken under humid conditions. Therefore, the water resistance of adhesives played a crucial role in their adhesion performance.[41] As shown in Fig. 6a, after adding SE, the insoluble fraction increased from 3% to 59.09%, while the addition of BHTA and M-CNC further increased the insoluble fraction of the adhesive, which was attributed to a decrease in the number of hydrophilic groups, a higher degree of crosslinking and thus a denser three-dimensional network with better water resistance.

Meanwhile, due to the increase in crosslinking degree and the formation of metal coordination between M-CNC and SPI, the thermal stability of M-CNC/B/SE/SPI was significantly improved.[7] In the thermogravimetric analysis (TGA) curve (Fig. 6b), it could be seen that the residual mass of M-CNC/B/SE/SPI at 600 ℃ was 55.45%, which was 17.62% higher than that of SPI (37.83%). The TGA curves of the adhesives exhibited two main degradation processes. The first stage from 100 ℃ to 260 ℃ was related to the destruction of unstable chemical interactions and the evaporation of internal bound water. The second stage from 260 ℃ to 550 ℃ was attributed to the break of covalent bonds (C-C, C-O, C-N) and the decomposition of peptide skeleton. The pyrolysis rate of M-CNC/B/SE/SPI was the lowest in these two stages, and the peak degradation rate of pristine SPI and M-CNC/B/SE/SPI appeared at 312 ℃ and 327 ℃, respectively, indicating a significant improvement in its thermal stability.[42]

3.9 Shear strength of adhesive

The adhesion properties of the adhesives were shown in Fig. 7. The dry shear strength of the original adhesive was 2.15 MPa. After adding SE, SE and SPI underwent a cross-linking reaction, forming a more compact network structure. The cohesion was enhanced, and the dry shear strength increased to 2.87 MPa. The wet shear strength was also increased from 0.62 MPa to 0.78 MPa. The addition of BHTA formed a multiple cross-linking network, making the adhesive structure more compact. The wet shear strength was enhanced to 0.82 MPa. After the addition of M-CNC, the hydrophilic groups of protein molecules chelated calcium ions, forming a stable mineralized skeleton that maintained high strength and rigidity

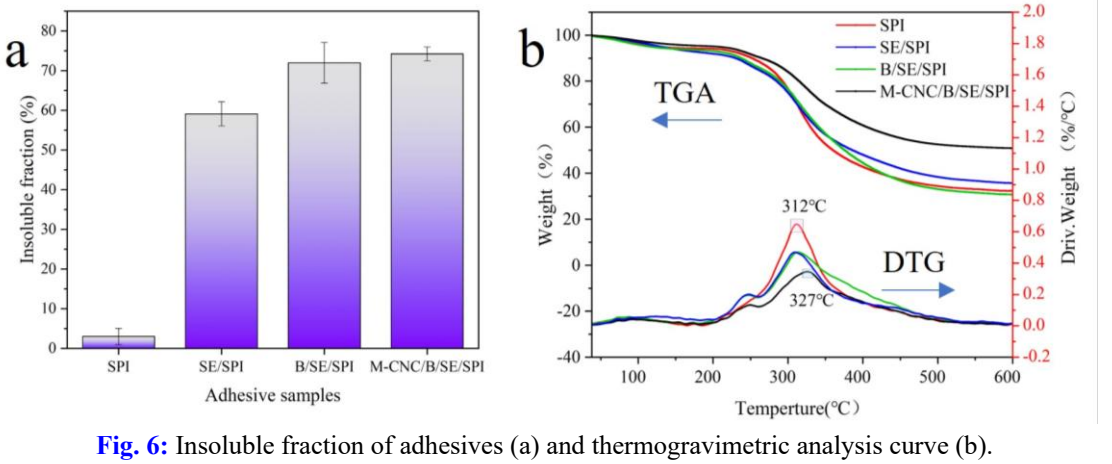

Fig. 6: Insoluble fraction of adhesives (a) and thermogravimetric analysis curve (b).

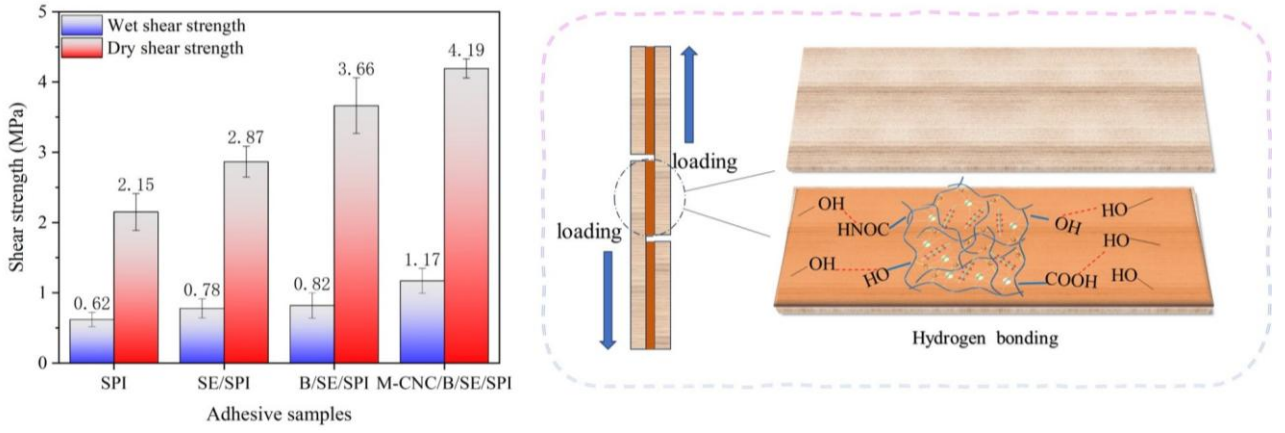

Fig. 7: Dry shear strength and wet shear strength of adhesives.

under humid conditions.[17] M-CNC/B/SE/SPI adhesive reached the maximum dry shear strength and wet shear strength of 4.19 and 1.17 MPa, respectively, which was beyond the Chinese National Standard for Class II of 0.7 MPa (GB/T17657−2013).

3.10 The antimildew and antifungal effect of adhesives

The mold resistance of adhesives was important for plywood storage and industrial applications. SPI adhesives were prone to spoilage and mold, which could reduce their adhesion and spreading ability.[40] As shown in Fig. 8, after being placed at 30 °C and 75% RH for 72 h, SPI was infected with mold, showing obvious discoloration, deterioration, and emitting a foul odor. Due to the antimold properties of SE, it had a protective effect on SPI. SE/SPI and showed partial moldy growth. The synergistic effect of imine linkages in BHTA and SE enhanced the anti-mold activity of B/SE/SPI, M-CNC/B/SE/SPI, and after 72 h, there was basically no mold infection.[43]

In the study, the effects of adhesives on white rot fungi and Trichoderma were further evaluated. The addition of SE significantly increased the growth inhibition rate of adhesive on white rot fungus and *Trichoderma harzianum* by 51.00% and 30.93%, respectively, compared to that of pristine SPI. The addition of BHTA had no effect on the growth inhibition rate of white rot fungi and *Trichoderma harzianum*. The addition of M-CNC increased the growth inhibition rates of adhesive against white rot fungus and *Trichoderma harzianum* to 58.12% and 48.33%, respectively (Fig. 9). Based on the above results, it could be seen that the adhesive itself had the effect of antimold and and antifungal properties, which could provide plywood with anti-decay effect.

3.11 The effect of adhesives on the mechanical properties of plywood

The static bending strength of plywood was measured using the three-point bending method, and the influence of different adhesives on the mechanical properties of plywood was explored. When subjected to 200 g loading, the piled veneers deformed apparently, while the plywood had almost no deformation (Fig. 10d). As shown in Fig. 10c, the mechanical property of the piled veneers was poor, with a static bending strength of 5.68 MPa. The mechanical performance of plywood prepared by SPI adhesive was improved, and the static bending strength has been increased to 14.01MPa. The plywood prepared with M-CNC/B/SE/SPI adhesive had the

Fig. 8: Digital photos of the adhesives in their original state and after 72 h of storage.

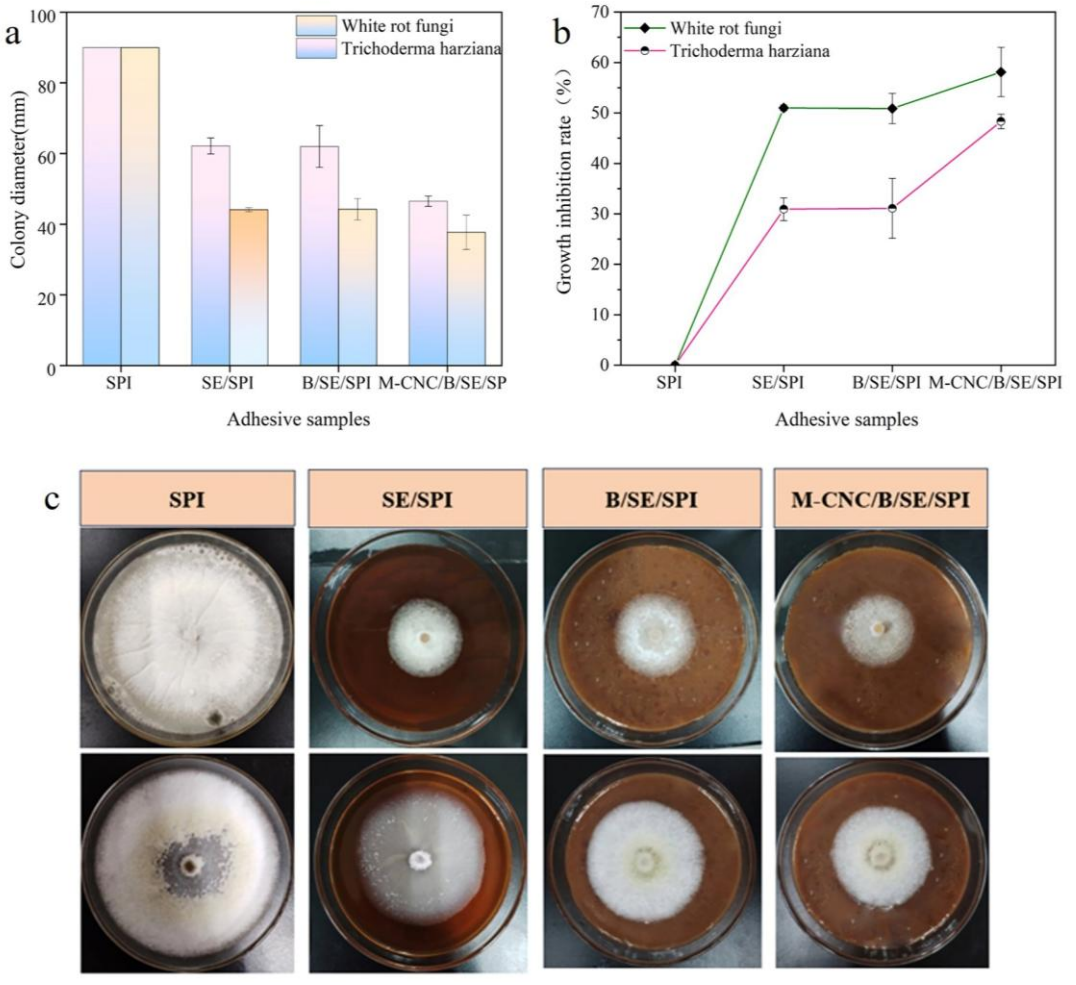

Fig. 9: Colony diameter of white rot fungus and *Trichoderma* on mixed adhesive culture medium (a), growth inhibition rate (b), and growth status of white rot fungus and *Trichoderma* (c).

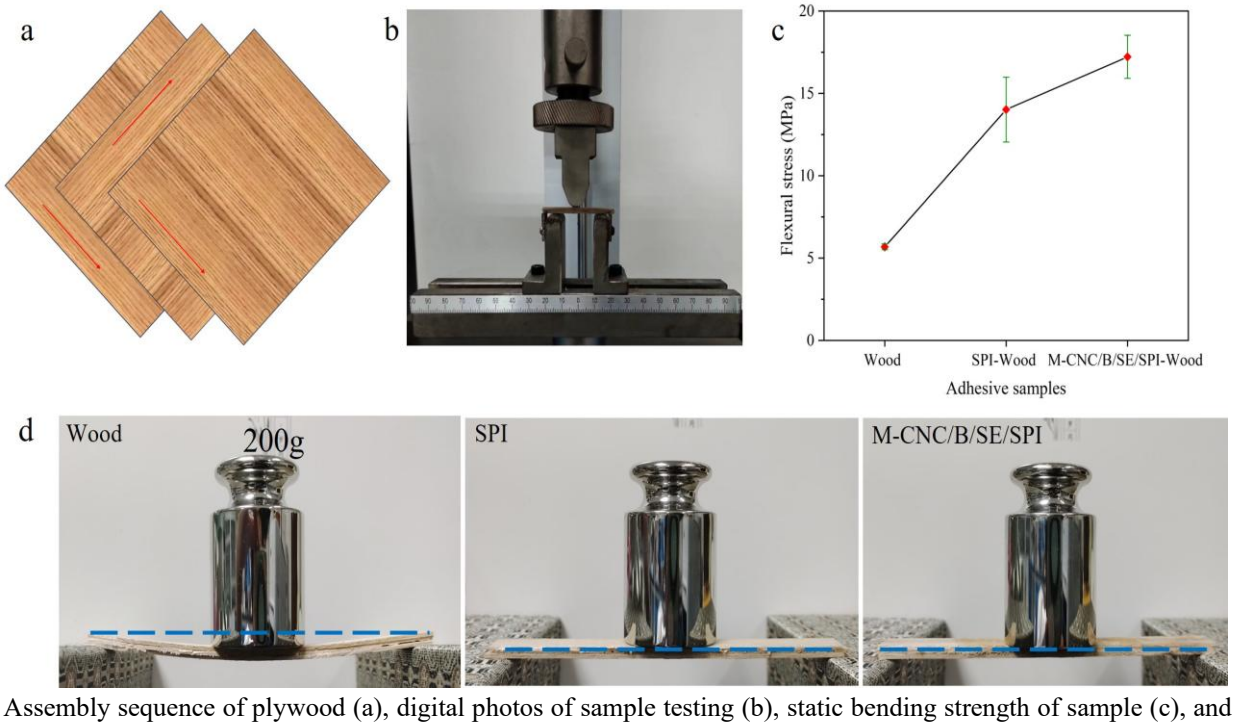

Fig. 10: Assembly sequence of plywood (a), digital photos of sample testing (b), static bending strength of sample (c), and state of sample under stress (d).

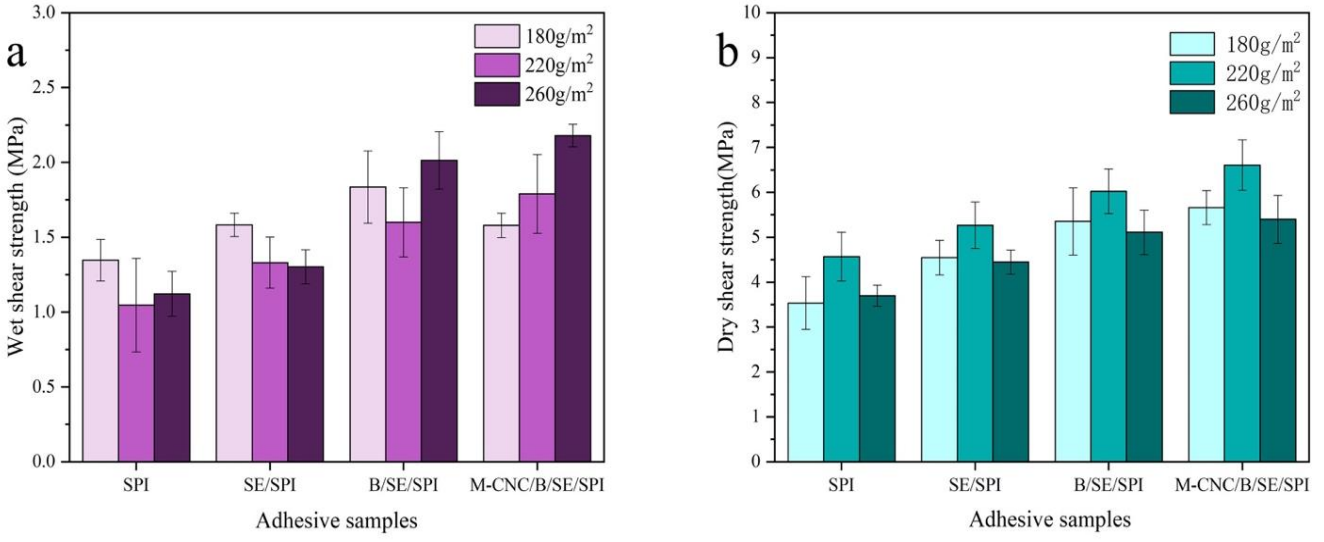

Fig. 11: The shear strength of plywood prepared with different adhesive consumption (a) wet shear strength and (b) dry shear strength.

highest static bending strength of 17.22 MPa. M-CNC/B/SE/SPI adhesive could significantly improve the mechanical properties of the plywood.

This study further investigates the influence of hot-pressing temperature and adhesive consumption on the bonding strength of modified adhesives. At an adhesive consumption of 260 g/m^2, the wet bonding strength of M-CNC/B/SE/SPI can exceed 2 MPa (Fig. 11a). However, the dry shear strength is generally superior at an adhesive consumption of 220 g/m² compared to both 180 g/m² and 260 g/m² (Fig. 11b). It is likely that excessive adhesive application leads to suboptimal curing and heat transfer effects under identical hot-pressing conditions. Furthermore, practical observations revealed that samples with higher adhesive consumption tended to be extruded during hot pressing, resulting in gaps along some wood edges; this diminished the actual bonding area relative to the intended area, thereby reducing overall bonding strength.

As illustrated in Fig. 12b, an increase in hot-press temperature correlates with a rise in the dry shear strength of plywood. Elevated temperatures disrupt the conformation of SPI, facilitating more comprehensive reactions among SE, BHTA, M-CNC, and SPI molecules. This results in enhanced molecular bonding and a denser three-dimensional network structure, thereby improving the bonding strength of the plywood. The overall trend observed for wet shear strength mirrors that of dry shear strength (Fig. 12a).

3.12 Comprehensive performance comparison

Compared with representative bio-based adhesives reported in recent years (Table 2), M-CNC/B/SE/SPI adhesive had excellent comprehensive properties such as high bonding strength, mold resistance, antifungal effect, and enhanced mechanical strength of plywood. Therefore, using *Stellera chamaejasme* plant extracts to construct multiple cross-linked and biomineralized structures provided a new approach for developing powerful biomass-derived adhesives and achieving high-value utilization of plants.

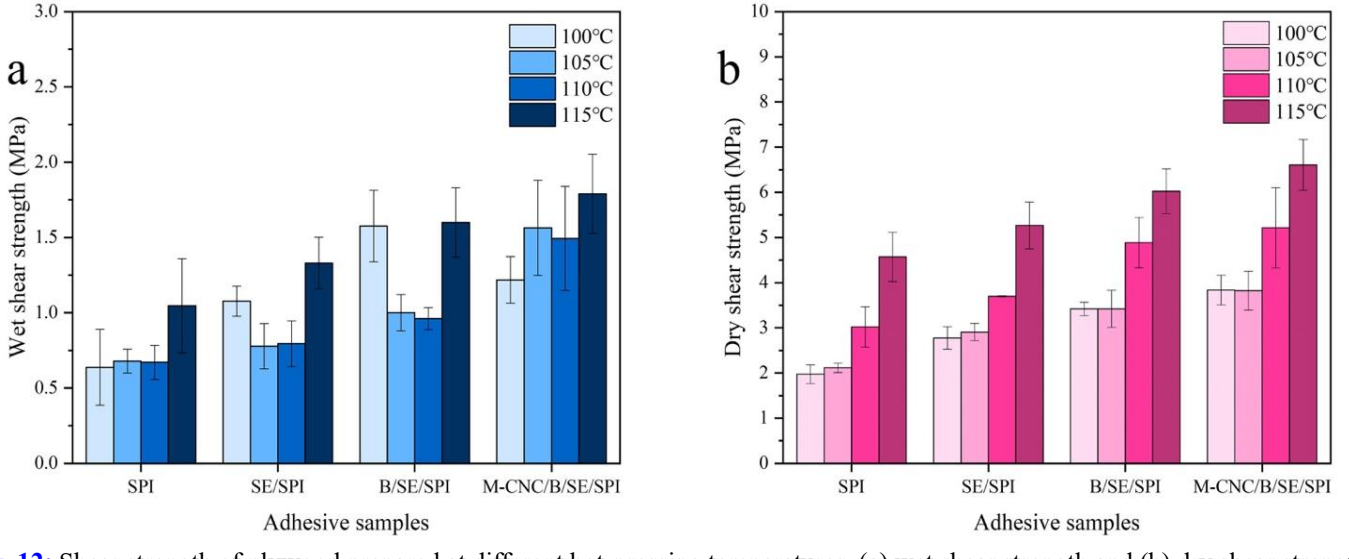

Fig. 12: Shear strength of plywood prepared at different hot-pressing temperatures, (a) wet shear strength and (b) dry shear strength.

Table 2: Comprehensive performance comparison between M-CNC/B/SE/SPI adhesive and representative bio-based adhesives reported in recent years.

Soy-based adhesive	Wet shear strength (MPa)	Dry shear strength (MPa)	Anti-mold time (Days)	growth inhibition rate%	mechanical properties of plywood	Pressing pressure, temperature and time	Reference
M-CNC/B/SE/SPI	1.17	4.19	3	58.12	17.22	1.5MPa 105 ℃ 180s	This work
SP/PUSD	1.74	3.03	/	/	/	1MPa 120 ℃ 315s	[36]
SPAE(polyamidoamine-epichlorohydrin)-FA(folicacid)-$CaCO_3$	0.96	1.73	/	/	/	1MPa 120 ℃ 315s	[38]
SM/TCu(CuSO4, tannin) /HBSi(hyper-branched silicone)	1.27	1.98	/	/	/	1MPa 120 ℃	[7]
HSM/PAE(thiol-grafted polyamide-epichlorohydrin)-SH/LS(lignosulfonate)	1.41	2.82	10	/	/	1MPa 120 ℃ 315s	[42]
SP/OCNF(Oxidation of Carboxymethylated CNFs)-CA	1.35	4.21	/	/	/	1MPa 120 ℃ 300s	[44]
SP/AA(acrylic acid)/CSA(calcium sulfoaluminate)	1.21	2.03	15	/	/	1MPa 120 ℃ 315s	[45]
SM/CS/CT@BNNSs(catechol-rich condensed tannin-functionalized boron nitride nanosheets)	1.46	2.38	/	/	/	1MPa 120 ℃ 330s	[16]
SPI/DDE(daidzein)	1.56	2.3	5	/	/	1MPa 120 ℃ 360s	[40]
SF/pAS@CNF(pDA/ASC-functionalized CNF)	1.53	4.6	/	/	/	1MPa 120 ℃ 315s	[46]
SM/MCF/LAQ@AC(cationic long-alkyl-chain quaternary salt)	1.87	2.58	3	/	/	1MPa 120 ℃ 360s	[17]
SPI/Tannin	0.81	1.3	/	/	/	1.1MPa 160 ℃ 660s	[35]
SP/o-DP@MMT(phenolic polymer, montmorillonite)	0.84	1.95	12	/	/	1MPa 120 ℃ 360s	[47]
SF/UF(urea-formaldehyde)	1.23	2.17	/	/	/	1.5MPa 130 ℃ 300s	[2]
Tannin	0.57	1.69	/	/	/	1.75MPa 160 ℃ 180s	[48]

4. Conclusion

This study prepared an antimold, antifungal and thermally stable biomass-derived adhesive M-CNC/B/SE/SPI with excellent adhesion property using active substances from the roots of *Stellera chamaejasme*, mineralized cellulose nanocrystals, and SPI as raw materials. Compared with pure SPI, the dry shear strength of the modified adhesive increased from 2.15 MPa to 4.19 MPa, which was higher than most of SPI based adhesives. The wet shear strength was1.17MPa, which was 88.72% higher than that of SPI and met the national requirements for Class II plywood (GB/T17657-2013). This was mainly due to the synergistic effects of hydrogen bonds, covalent bonds, and metal coordination. Besides, the antimold and antifungal activity of the adhesive was improved by the inherently antimold properties of flavonoids, coumarins, and other active substances in *Stellera chamaejasme* root extract as well as imine linkages of BHTA and positively charged M-CNC. M-CNC/B/SE/SPI was expected to have greatly extended shelf life of 72 h. Its growth inhibition rates against white rot fungi and trichoderma were 58.12% and 48.33%, respectively. Futhermore, the fabrication process of M-CNC/B/SE/SPI adhesive was facile, green and scalable. Therefore, the novel and sustainable strategy proposed in this article would provide potential high-performance, environmentally friendly biomass-derived adhesives in industrial production and applications.

Acknowledgement

Min Pan and Shuliang Li contributed equally to this work. Additionally, the authors acknowledge China-Portugal Joint Laboratory of Cultural Heritage Conservation Science supported by the Belt and Road Initiative. The authors are very grateful for financial support from National Natural Science Foundation of China (22376173), Sichuan Provincial Youth Scientific and Technological Innovation Research Team on Ecological Adaptability of Plateau Architecture (2022JDTD0008), Chengdu Science and Technology Project (2024-YF05- 00889-SN), Natural Science Foundation of

Sichuan Province (2024NSFSC0994) and the Project of Qinghai-Tibetan Plateau Research in Southwest Minzu University (2024CXTD06).

Conflict of Interest

There is no conflict of interest.

Supporting Information

Applicable.

References

[1] H. Chen, S. S. Nair, P. Chauhan, N. Yan, Lignin containing cellulose nanofibril application in pMDI wood adhesives for drastically improved gap-filling properties with robust bondline interfaces, *Chemical Engineering Journal*, 2019, **360**, 393-401, doi: 10.1016/j.cej.2018.11.222.

[2] S. B. Hosseini, M. Asadollahzadeh, S. Kazemi Najfai, M. J. Taherzadeh, Partial replacement of urea-formaldehyde adhesive with fungal biomass and soy flour in plywood fabrication, *Journal of Adhesion Science and Technology*, 2020, **34**, 1371-1384, doi: 10.1080/01694243.2019.1707948.

[3] Y. Li, L. Cai, H. Chen, Z. Liu, X. Zhang, J. Li, S. Q. Shi, J. Li, Q. Gao, Preparation of a high bonding performance soybean protein-based adhesive with low crosslinker addition via microwave chemistry, *International Journal of Biological Macromolecules*, 2022, **208**, 45-55, doi: 10.1016/j.ijbiomac.2022.03.059.

[4] G. Xu, Q. Zhang, X. Xi, H. Lei, M. Cao, G. Du, Z. Wu, Tannin-based wood adhesive with good water resistance crosslinked by hexanediamine, *International Journal of Biological Macromolecules*, 2023, **234**, 123644, doi: 10.1016/j.ijbiomac.2023.123644.

[5] Z. Zhang, Composites Part B-special issue: alkali activated materials and composites, *Composites Part B: Engineering*, 2023, **257**, 110690, doi: 10.1016/j.compositesb.2023.110690.

[6] Y. Zeng, W. Yang, P. Xu, X. Cai, W. Dong, M. Chen, M Du, T. Liu, P. Jan Lemstra, P. Ma, The bonding strength, water resistance and flame retardancy of soy protein-based adhesive by incorporating tailor-made core–shell nanohybrid compounds, *Chemical Engineering Journal*, 2022, **428**, 132390, doi: 10.1016/j.cej.2021.132390.

[7] S. Jin, K. Li, Q. Gao, W. Zhang, H. Chen, J. Li, S. Q. Shi, Multiple crosslinking strategy to achieve high bonding strength and antibacterial properties of double-network soy adhesive, *Journal of Cleaner Production*, 2020, **254**, 120143, doi: 10.1016/j.jclepro.2020.120143.

[8] Z. Liu, T. Liu, W. Gu, X. Zhang, J. Li, S. Q. Shi, Q. Gao, Hyperbranched catechol biomineralization for preparing super antibacterial and fire-resistant soybean protein adhesives with long-term adhesion, *Chemical Engineering Journal*, 2022, **449**, 137822, doi: 10.1016/j.cej.2022.137822.

[9] Q. Yan, Y. Sun, Z. Li, Y. Zhu, S. Zhang, Excellent strength and toughness and multifunctional protein-based adhesive produced by polyether block sulfuretted polyamidoamine-epichlorohydrin via a dual-crosslinking strategy, *Industrial Crops and Products*, 2023, **203**, 117083, doi: 10.1016/j.indcrop.2023.117083.

[10] Z. Sun, B. Sun, Y. Bai, Z. Gao, Economical improvement on the performances of a soybean flour-based adhesive for wood composites via montmorillonite hybridization, *Composites Part B: Engineering*, 2021, **217**, 108920, doi: 10.1016/j.compositesb.2021.108920.

[11] C. Ma, H. Pang, Y. Shen, W. Ji, S. Zhang, Oyster-inspired organic-inorganic hybrid system to improve cold-pressing adhesion, flame retardancy, and mildew resistance of soybean meal adhesive, *Composites Part B: Engineering*, 2022, **242**, 110049, doi: 10.1016/j.compositesb.2022.110049.

[12] M. Swadźba-Kwaśny, P. Licence, *ACS sustainable chemistry & engineering* virtual special issue on advanced reaction media, *ACS Sustainable Chemistry & Engineering*, 2019, **7**, 12638, doi: 10.1021/acssuschemeng.9b04069.

[13] E. Averina, J. Konnerth, S. D'Amico, H. W. G. van Herwijnen, Protein adhesives: alkaline hydrolysis of different crop proteins as modification for improved wood bonding performance, *Industrial Crops and Products*, 2021, **161**, 113187, doi: 10.1016/j.indcrop.2020.113187.

[14] S. Yao, B. Jin, Z. Liu, C. Shao, R. Zhao, X. Wang, R. Tang, Biomineralization: from material tactics to biological strategy, *Advanced Materials*, 2017, **29**, 1605903, doi: 10.1002/adma.201605903

[15] F. Zhang, G. Zeng, Y. Zhou, X. Li, Y. Dong, Y. Cai, J. Li, J. Li, Z. Fang, Green and efficient production of functionalized graphene to achieve soybean meal-based adhesive enhancement, *Journal of Cleaner Production*, 2022, **376**, 134068, doi: 10.1016/j.jclepro.2022.134068.

[16] Y. Chen, Y. Lyu, X. Yuan, X. Ji, F. Zhang, X. Li, J. Li, X. Zhan, J. Li, A biomimetic adhesive with high adhesion strength and toughness comprising soybean meal, chitosan, and condensed tannin-functionalized boron nitride nanosheets, *International Journal of Biological Macromolecules*, 2022, **219**, 611-625, doi: 10.1016/j.ijbiomac.2022.08.028.

[17] K. Li, S. Jin, X. Li, J. Li, S. Q. Shi, J. Li, Bioinspired interface engineering of soybean meal-based adhesive incorporated with biomineralized cellulose nanofibrils and a functional aminoclay, *Chemical Engineering Journal*, 2021, **421**, 129820, doi: 10.1016/j.cej.2021.129820.

[18] Y. Zhang, Z. Liu, Y. Xu, J. Li, S. Q. Shi, J. Li, Q. Gao, High performance and multifunctional protein-based adhesive produced via phenol-amine chemistry and mineral reinforcement strategy inspired by arthropod cuticles, *Chemical Engineering Journal*, 2021, **426**, 130852, doi: 10.1016/j.cej.2021.130852.

[19] G. Strauss, S. M. Gibson, Plant phenolics as cross-linkers of gelatin gels and gelatin-based coacervates for use as food ingredients, *Food Hydrocolloids*, 2004, **18**, 81-89, doi: 10.1016/s0268-005x(03)00045-6.

[20] Y. Cao, Y. L. Xiong, Chlorogenic acid-mediated gel formation of oxidatively stressed myofibrillar protein, *Food Chemistry*, 2015, **180**, 235-243, doi: 10.1016/j.foodchem.2015.02.036.

[21] B. Feng, Y. Pei, H. Hua, T. Wang, Y. Zhang, Biflavonoids from stellera chamaejasme, *Pharmaceutical Biology*, 2003, **41**, 59-61, doi: 10.1076/phbi.41.1.59.14701.
[22] S. Jongberg, M. A. Tørngren, A. Gunvig, L. H. Skibsted, M. N. Lund, Effect of green tea or rosemary extract on protein oxidation in Bologna type sausages prepared from oxidatively stressed pork, *Meat Science*, 2013, **93**, 538-546, doi: 10.1016/j.meatsci.2012.11.005.
[23] C. X. Jing, J. J. Guo, B. J. Yang, S. R. Fan, Y. T. Wang, D. Z. Chen, X. J. Hao, Stelleraguaianone B and C, two new sesquiterpenoids from Stellera chamaejasme L., *Fitoterapia*, 2019, **134**, 443-446, doi: 10.1016/j.fitote.2019.03.024.
[24] X. Li, K. Rahman, J. Zhu, H. Zhang, Chemical constituents and pharmacological activities of stellera chamaejasme, *Current Pharmaceutical Design*, 2018, **24**, 2825-2838, doi: 10.2174/1381612824666180903110802.
[25] J. Li, Q. Shen, C. H. Bao, L. T. Chen, X. R. Li, A new dicoumarinyl ether from the roots of Stellera chamaejasme L, *Molecules*, 2014, **19**, 1603-1607, doi: 10.3390/molecules19021603.
[26] G. Gu, M. Jiang, H. Hu, W. Qiao, H. Jin, T. Hou, K. Tao, Neochamaejasmin B extracted from Stellera chamaejasme L. induces apoptosis through caspase-10-dependent way in insect neuronal cells, *Archives of Insect Biochemistry and Physiology*, 2022, **110**, e21892, doi: 10.1002/arch.21892.
[27] M. Wu, J. Shao, J. Zhu, J. Zi, Chamaejasnoids A-E, a 2,3-seco-guaiane sesquiterpenoid with a 5/6/7 bridged ring system and related metabolites from Stellera chamaejasme L., *Fitoterapia*, 2022, **158**, 105171, doi: 10.1016/j.fitote.2022.105171.
[28] Q. Zhang, Y. Du, Z. Cheng, X. Huang, S, Song, Studies on the Chemical Components and Biological Activities of Stellera chamaejasme L, *Asian Journal Of Traditional Medicines*, 2018, **13**, 49-59, doi: CN/Y2018/V13/I1/49.
[29] X. Liu, Q. Yang, G. Zhang, Y. Li, Y. Chen, X. Weng, Y. Wang, Y. Wang, X. Zhu, Anti-tumor pharmacological evaluation of extracts from stellera chamaejasme L based on hollow fiber assay, *BMC Complementary and Alternative Medicine*, 2014, **14**, 116, doi: 10.1186/1472-6882-14-116.
[30] Y. Zeng, P. Xu, W. Yang, H. Chu, W. Wang, W. Dong, M. Chen, H. Bai, P. Ma, Soy protein-based adhesive with superior bonding strength and water resistance by designing densely crosslinking networks, *European Polymer Journal*, 2021, **142**, 110128, doi: 10.1016/j.eurpolymj.2020.110128.
[31] Z. Bi, F. Yang, Y. Lei, J. J. Morrell, L. Yan, Identification of antifungal compounds in konjac flying powder and assessment against wood decay fungi, *Industrial Crops and Products*, 2019, **140**, 111650, doi: 10.1016/j.indcrop.2019.111650.
[32] S. Ghahri, B. Mohebby, A. Pizzi, A. Mirshokraie, H. R. Mansouri, Improving water resistance of soy-based adhesive by vegetable tannin, *Journal of Polymers and the Environment*, 2018, **26**, 1881-1890, doi: 10.1007/s10924-017-1090-6.
[33] M. Chen, J. Luo, R. Shi, J. Zhang, Q. Gao, J. Li, Improved adhesion performance of soy protein-based adhesives with a larch tannin-based resin, *Polymers*, 2017, **9**, 408, doi: 10.3390/polym9090408.
[34] L. Wang, J. Liu, W. Zhang, D. Zhang, J. Li, S. Zhang, Biomimetic soy protein-based exterior-use films with excellent UV-blocking performance from catechol derivative Acacia mangium tannin, *Journal of Applied Polymer Science*, 2020, **138**, 50185, doi: 10.1002/app.50185.
[35] S. Ghahri, A. Pizzi, R. Hajihassani, A study of concept to prepare totally biosourced wood adhesives from only soy protein and tannin, *Polymers*, 2022, **14**, 61150, doi: 10.3390/polym14061150.
[36] S. Zhao, H. Pang, Z. Li, Z. Wang, H. Kang, W. Zhang, S. Zhang, J. Li, L. Li, Polyurethane as high-functionality crosslinker for constructing thermally driven dual-crosslinking plant protein adhesion system with integrated strength and ductility, *Chemical Engineering Journal*, 2021, **422**, 130152.
[37] S. Zhao, Y. Wen, Z. Wang, H. Kang, J. Li, S. Zhang, Y. Ji, Preparation and demonstration of poly(dopamine)-triggered attapulgite-anchored polyurethane as a high-performance rod-like elastomer to reinforce soy protein-isolated composites, *Applied Surface Science*, 2018, **442**, 537-546, doi: 10.1016/j.apsusc.2018.02.110.
[38] H. Pang, C. Ma, S. Zhang, Conversion of soybean oil extraction wastes into high-performance wood adhesives based on mussel-inspired cation-π interactions, *International Journal of Biological Macromolecules*, 2022, **209**, 83-92, doi: 10.1016/j.ijbiomac.2022.03.152.
[39] J. Zhang, C. Long, X. Zhang, Z. Liu, X. Zhang, T. Liu, J. Li, Q. Gao, An easy-coating, versatile, and strong soy flour adhesive via a biomineralized structure combined with a biomimetic brush-like polymer, *Chemical Engineering Journal*, 2022, **450**, 138387, doi: 10.1016/j.cej.2022.138387.
[40] C. Xu, Y. Yu, M. Chen, Y. Zhang, J. Li, Q. Gao, S. Q. Shi, Soy protein adhesive with bio-based epoxidized daidzein for high strength and mildew resistance, *Chemical Engineering Journal*, 2020, **390**, 124622, doi: 10.1016/j.cej.2020.124622.
[41] M. Liu, Y. Wang, Y. Wu, Z. He, H. Wan, "Greener" adhesives composed of urea-formaldehyde resin and cottonseed meal for wood-based composites, *Journal of Cleaner Production*, 2018, **187**, 361-371, doi: 10.1016/j.jclepro.2018.03.239.
[42] Q. Yan, C. Ma, Z. Liang, S. Zhang, High-temperature soybean meal adhesive based on disulfide bond rearrangement and multiple crosslinking: water resistance and prepressing adhesion, *Journal of Cleaner Production*, 2022, **373**, 133709, doi: 10.1016/j.jclepro.2022.133709.
[43] J. Peng, S. Xie, T. Liu, D. Wang, R. Ou, C. Guo, Q. Wang, Z. Liu, High-performance epoxy vitrimer with superior self-healing, shape-memory, flame retardancy, and antibacterial properties based on multifunctional curing agent, *Composites Part B: Engineering*, 2022, **242**, 110109, doi: 10.1016/j.compositesb.2022.110109.
[44] Z. Wang, H. Kang, H. Liu, S. Zhang, J. Li, Dual-Network Nanocross-linking Strategy to Improve Bulk Mechanical and Water-Resistant Adhesion Properties of Biobased Wood Adhesives, *ACS Sustainable Chemistry & Engineering*, 2020, **8**, 16430-164407, doi: 10.1021/acssuschemeng.0c04913.

[45] H. Pang, C. Ma, Y. Shen, Y. Sun, J. Li, S. Zhang, L. Cai, Z. Huang, Novel bionic soy protein-based adhesive with excellent prepressing adhesion, flame retardancy, and mildew resistance, *ACS Applied Materials & Interfaces*, 2021, **13**, 38732-38744, doi: 10.1021/acsami.1c11004.
[46] Z. Wang, S. Zhao, W. Zhang, C. Qi, S. Zhang, J. Li, Bio-inspired cellulose nanofiber-reinforced soy protein resin adhesives with dopamine-induced codeposition of "water-resistant" interphases, *Applied Surface Science*, 2019, **478**, 441-450, doi: 10.1016/j.apsusc.2019.01.154.
[47] Y. Zhang, Z. Liu, Y. Xu, J. Li, S. Q. Shi, J. Li, Q. Gao, High performance and multifunctional protein-based adhesive produced via phenol-amine chemistry and mineral reinforcement strategy inspired by arthropod cuticles, *Chemical Engineering Journal*, 2021, **426**, 130852, doi: 10.1016/j.cej.2021.130852.
[48] X. Xi, A. Pizzi, C. R. Frihart, L. Lorenz, C. Gerardin, Tannin plywood bioadhesives with non-volatile aldehydes generation by specific oxidation of mono- and disaccharides, *International Journal of Adhesion and Adhesives*, 2020, **98**, 102499, doi: 10.1016/j.ijadhadh.2019.102499.